Economic Evaluation of a Hybrid Hydrogen Liquefaction System Utilizing Liquid Air Cold Recovery and Renewable Energies

M. Taghavi[1], H. Salarian[1*] and B. Ghorbani[2]

1. Department of Mechanical Engineering, Nour Branch, Islamic Azad University, Nour, Iran.
2. Faculty of Engineering Modern Technologies, Amol University of Special Modern Technologies, Amol, Iran.

Abstract
Liquefaction systems are among the physical techniques of hydrogen (H_2) storage with a high specific power consumption (SPC), a high manufacturing cost, and inevitable boil-off losses. Liquid air cold (LAC) recovery is among the strategies that could be used to reduce the energy consumption of these systems. The present work economically evaluates a combined hydrogen liquefaction configuration using combined heat and power (CHP) system, photovoltaic cell (PVC) unit, and liquid air energy recovery for pre-cooling under climatic states of Yazd, Iran. The LAC recovery is used to pre-cool hydrogen. Moreover, the cascade refrigeration systems with helium and hydrogen refrigerants are employed to supply refrigeration and liquefaction. Liquid air along with natural gas enters CHP after cold energy recovery and compression, and supplies a part of the power demand of the liquefaction structure. The rest of the power required for refrigeration cycles to liquefy hydrogen is supplied by the PVC unit. This integrated structure generates liquid hydrogen by receiving 5559 kW of power from PVC unit, 60.79 kg/h of natural gas, 8000 kg/h of liquid air, and 1028 kg/h of gaseous hydrogen as the inputs. The annualized cost of the configuration (ACC) is applied to economically evaluate the hydrogen liquefaction system using renewable energies. The developed integrated structure is economically evaluated by the HYSYS V10 software and the m-file code in the MATLAB package. The economic research results of the hybrid cycle indicate the period of return (POR), prime price of liquid hydrogen production, and additive value (AV) are 4.249 years, 5.432 USD/kg LH_2, and 1.567 USD/kg LH_2, respectively. The economic sensitivity examination of the combined system reveals POR increases from 2.295 to 13.97 years and net annual profit decreases from 32.66 to 5.366 MMUSD/year by increasing the gaseous hydrogen cost from 1.4 to 3.4 USD/kg LH_2. Moreover, POR increases from 2.753 to 25.07 years, and the levelized cost of product increases from 5.02 to 7.488 US$/kg LH_2 by increasing the capital cost from 52.5 to 217.5 MMUSD.

1. Introduction

The growing population, declining fossil fuels, and increasing pollution from these energy sources have recently led the researchers to consider other energy sources that are both clean and sustainable. Therefore, hydrogen can be considered as an important energy carrier and a suitable alternative for fossil fuels [1]. The hydrogen energy density plays a major role in hydrogen distribution and transportation. Hydrogen has a low energy density despite its high heating value. Hydrogen has a significantly lower energy density compared to the fossil fuels. The energy density of the compressed H_2 is approximately 17 times inferior to that of liquid

gasoline at 200 bar and 15 °C. However, its energy density can significantly increase by liquefaction. Studies have reported that the energy density of liquid hydrogen is 5 times higher than that of the compressed state at 200 bar and 15 °C [2]. The hydrogen liquefaction method is used for long-term hydrogen storage and transport to distant places. The reduced specific energy consumption (SEC) for H_2 liquefaction has recently received a great attention [3]. Cryogenic liquids, nanomaterials, chemical hydrides, metal hydrides, and compressed gas are used as the hydrogen storage systems [4].

1.1. Hydrogen liquefaction cycle

Hydrogen passes through other parts to reach a high pressure and a temperature close to the normal boiling point. The current state of the gas along with final expansion leads to hydrogen liquefaction. This expansion can occur due to enthalpy at Joule-Thomson valve or entropy in wet expanders. In the hydrogen liquefaction process, temperature decreases through pre-cooling and cryogenic cooling [5].

1.2. Photovoltaic

Solar energy is among the most sustainable and cheap energy sources in the world. Generating electricity by PV systems is among the main applications of solar energy. Using solar energy and PVC units have recently received a great attention [6]. Yazd has approximately 330 sunny days per year and a good renewable energy capacity. In this work, electricity is generated considering the geographical location and weather conditions of Yazd as well as using solar energy and PV systems to supply a part of the cycle demand.

1.3. Combined heat and power system

A fuel cell is an electro-chemical unit that changes the chemical energy resulting from a chemical reaction into useful electrical energy. Nowadays, fuel cells are regarded as a novel technology in energy production, among which solid oxide fuel cells (SOFCs) have received a greater attention owing to high efficiency, lack of environmental pollution, combined heat and power generation, ability to use different fuels including hydrogen and capability of hybrid with other units [7]. The energy conversion efficiency of this system is very high, and its waste is very low or zeroes depending on the type of fuel consumed. Moreover, the heat produced in these fuel cells is of high quality, and could be used in various power generation systems. The hybrid systems developed by combining SOFCs with different power generation systems have received a great attention as novel energy generation sources. Due to their high efficiency and low pollutant emission, these hybrid systems could significantly affect power generation in the near future. Hydrogen fuel cells do not emit any pollution, and their only by-product is pure water vapor [8].

1.4. Literature review

Naquash *et al*. [9] have examined the performance of the integrated H_2 liquefaction system using the ORC-based liquid air energy system and absorption refrigeration. The results indicated that the SEC and exergy efficiency were obtained at 6.71 kWh/kg LH_2 and 35.7%. Taghavi *et al*. [5] have developed a combined H_2 liquefaction configuration by the LAE recovery, PVC units, and fuel cell. The results revealed that the hybrid structure generated 1028 kg/h of liquid hydrogen. The power generation cycle efficiency, the SPC of H_2 liquefaction process, and fuel cell system efficiency were obtained as 44.06%, 5.955 kWh/kg LH_2, and 62.96%, respectively. Riaz *et al*. [10] have examined the feasibility of improving the performance of liquefied natural gas (LNG) regasification in the H_2 liquefaction system using the exergy and energy analyses. The results obtained revealed that the total amount of refrigerant decreased by approximately 50%. Moreover, the exergy efficiency of the developed process was calculated at 42.25%. Wilhelmsen *et al*. [11] have tried to reduce exergy destruction in low-temperature exchangers in H_2 liquefaction system. They proposed a novel model of plate-fin exchanger for H_2 liquefaction. The potential of the developed model for reducing exergy destruction was obtained as 43%. Nabat *et al*. [12] have examined a novel energy storage system by liquid air energy storage (LAES). They integrated LAES with high-temperature thermal energy storage (HTES) by performing energy, exergy, and economic analyses. The round-trip exergy and energy efficiencies were calculated at 52.84% and 61.13%, respectively. Yuksel *et al*. have suggested a novel integrated cycle for H_2 liquefaction and production using waste material gasification [13]. The proposed integrated system was examined by the exergy and energy analyses. The results obtained revealed that the hydrogen production rate and total exergy and energy efficiencies were obtained as 0.077 kg/s, 58.15%, and 61.57%, respectively, when the generated net power was 94 MW. Naquash *et al*. have presented a novel method in order to improve the efficiency of the H_2 liquefaction system [14]. Carbon dioxide was used as the pre-cooling refrigerant. The exergy, energy, and economic analyses were considered. The results obtained indicated that the exergy efficiency of the proposed process was 31.4%, and hydrogen could be liquefied at the expense of 7.63 kWh/kg. Kaşka *et al*. have evaluated the efficiency of the hybrid organic Rankine-vapor compression cooling plant by H_2 liquefaction [15]. The efficiency coefficient of the whole system was calculated considering the first and second laws. The results obtained showed that the hydrogen liquefaction cost was 0.995 USD/kg H_2. Yang *et al*. [16] have proposed a combined H_2

liquefaction model by steam methane reforming (SMR). They designed their model using a LNG cooling system, and analyzed the techno-economic performance of the H_2 liquefaction system. The simulation results revealed that the energy required for hydrogen liquefaction decreased from 13.58 to 11.05 kWh/kg. Khoshgoftar Manesh et al. [17] have analyzed the energy and exergy of a novel energy storage system by integrating the liquid air unit, Linde-Hampson liquefaction system, ORC, and molten carbonate fuel cell (MCFC). The results displayed that the storage and round-trip yields of hybrid system were 0.8622 and 0.6931, respectively. The exergy yields of the structure was calculated as 0.6025. Koc et al. [18] have thermodynamically evaluated a novel electricity energy cycle to produce liquid H_2. The useful production efficiency was examined using a thermodynamic approach under different working conditions, and energy and exergy analyses were performed. The exergy and energy efficiencies were obtained as 58.37% and 60.14%, respectively. Bi et al. [19] have analyzed and optimized an innovative H_2 liquefaction system for circulating H_2 refrigeration. The exergy losses of the main devices and temperature curves were examined. Moreover, the performance of the suggested system was compared with other existing systems. The results obtained showed that the SEC, coefficient of performance (COP), and exergy yield were obtained as 7.041 kWh/kg LH_2, 0.1834, and 0.5413, respectively, assuming complete liquefaction of H_2. Zhang et al. [20] have designed a new H_2 liquefaction process, and analyzed its performance. The proposed model was developed based on the combination of the improved Claude precooling system with Joule-Brayton cooling system and mixed refrigerants. The COP, SEC, and exergy yield of the developed unit were obtained as 0.1574, 5.85 kWh/kg LH_2, and 55.30%, respectively. Faramarzi et al. [21] have suggested a novel H_2 liquefaction system based on the mixed refrigerant cycle and LNG cold energy. The exergy and economic investigations were performed. Then the suggested cycle was compared with the previous cycles. The results obtained revealed that SEC of the developed model was 19.90% lower than that of similar models. Moreover, the annual cost of the developed model was 13.43% lower than that of the initial model. Ebrahimi et al. [22] have studied the thermodynamic properties of a new H_2 liquefaction system using solar collectors and a thermo-electrochemical unit. The pinch method was used in multi-stream exchanger in order to

achieve the heat exchanger networks. The thermal efficiency and SEC of the integrated system were obtained as 71.4% and 7.6 kWh/kg LH_2, respectively. Lee et al. [23] have presented an integrated hydrogen liquefaction model by SMR and CO_2 liquefaction processes. For this purpose, the techno-economic analysis was performed to examine the feasibility of each process. The process flow conditions were optimized using the genetic algorithm. The results obtained indicated that the energy efficiency was improved by 47.4% by modifying the refrigeration cycle. Seyam et al. [24] have investigated a H_2 liquefaction model integrated with the geothermal system. The H_2 liquefaction system consisted of the hydrogen Claude and nitrogen precooling units. The SEC, exergy, and energy efficiencies were obtained as 6.47 kWh/kg LH_2, 63.7%, and 19.8%, respectively. Yuksel et al. [25] have evaluated a new H_2 liquefaction plant by examining the extent of degradation of each process and exergy efficiency. Moreover, they performed the parametric analysis to assess the system performance. The results obtained showed that the exergy and energy efficiencies of the proposed model were calculated at 57.13% and 70.12%, respectively. Hammad et al. [26] have thermodynamically analyzed an advanced hydrogen liquefaction system to make modifications, and improve the system. The energy and exergy efficiencies were calculated to evaluate the system performance. The exergy and energy yields of the proposed cycle were 11.5% and 15.4%, respectively. Cardella et al. [27] have proposed a suitable approach for stepwise implementation of large hydrogen liquefiers in a cost-effective manner. The novel liquefaction processes were optimized in terms of cost and efficiency. The results obtained showed that SEC was among 5.9 and 6.6 kWh/kg LH_2 within 5 years. Moreover, the specific liquefaction prices decreased by about 60% by increasing production from 5 to 50 tons per day. Kanoglu et al. [28] have presented a new integrated cycle for the H_2 liquefaction unit. The presented model was analyzed using geothermal energy in absorption pre-cooling and the laws of thermodynamics. The exergy efficiency and COP of the cycle were obtained as 67.9% and 0.016, respectively. Asadnia et al. [29] have designed a hybrid structure to purify a stream-containing hydrogen. The results obtained showed that the purity, recovery rate, and exergy yield of the developed system were 88.1%, 25.1% and 91.73%, respectively. Bian et al. [30] have presented a novel H_2 liquefaction system, and performed the

thermodynamic and economic analyses. The proposed model was designed with LNG regasification and dual-pressure Brayton cascade cycle. The exergy efficiency and losses of the proposed process were 47.0% and 12.36 MW, respectively. Yin *et al*. [31] have analyzed and optimized a novel hydrogen liquefaction cycle. They compared their proposed system with other existing systems, and used genetic algorithms to optimize their process. The SEC and exergy efficiency were obtained as 7.1329 kWh/kg LH$_2$ and 0.4941, respectively. Incer-Valverde *et al*. [32] have evaluated a large-scale hydrogen liquefaction system. The most important components from the thermodynamic, economic, and environmental viewpoints were examined. The exergy-based method was used to identify the system inefficiencies. The results obtained showed that the exergy efficiencies of the H$_2$ liquefaction system and electrolyzer were calculated as 42% and 47%, respectively. Yilmaz [33] evaluated a H$_2$ liquefaction cycle by geothermal energy. The optimum energy consumption of H$_2$ liquefaction was calculated. Moreover, the life cycle price analysis of the H$_2$ liquefaction system was investigated. The network requirement of the liquefaction cycle was calculated as 8.6 kWh/kg LH$_2$. Koc *et al*. [34] have proposed a novel liquid hydrogen production model using the solar and biomass energies. The thermodynamic analysis was performed to design a more efficient system. The exergy and energy yields of the proposed cycle were calculated as 54.18% and 58.43%, respectively. Krasae-in *et al*. [35] have simulated a small-scale H$_2$ liquefaction test rig using a mixed refrigerant (MR) system. Exergy analysis was performed to find out the MR system losses. The results obtained showed that the exergy yield of the MR cycle was 38.3%. Yuksel *et al*. have proposed a novel integrated multi-generation system based on solar energy for hydrogen production and liquefaction [36]. The energy and exergy efficiencies were as 62.35% and 65.17%, respectively. Ratlamwala *et al*. [37] have proposed a novel hybrid system based on renewable energies for hydrogen liquefaction using the PV/T energy, geothermal energy, and Linde-Hampson cycle. The exergy and energy efficiencies of the developed integrated system decreased from 0.21 to 0.13 and 0.059 to 0.037, respectively. Azizabadi *et al*. [38] have developed a new concept for H$_2$ liquefaction using waste heat of thermal power plants. The performance of the proposed model depended on the exhaust gases of turbines of the gas power plant. The results obtained showed that COP and SEC were calculated as 0.271 and 4.5 kWh.kg LH$_2^{-1}$, respectively. Utlu *et al*. [39] have performed the exergy investigation of an advanced H$_2$ liquefaction system using the cryogenic method. The results obtained showed that the total exergy efficiency of the H$_2$ liquefaction cycle was 32.22%. Moreover, the total exergy destruction of devices was calculated as 44,915 kW. Gadalla *et al*. [40] have presented an integrated H$_2$ liquefaction system based on triple-effect absorption chiller using geothermal energy and Linde-Hampson system, and evaluated its performance. The results obtained showed that the exergy and energy efficiencies of the proposed cycle decreased from 0.92 to 0.08 and 1.33 to 0.12, respectively. Ozcan *et al*. [41] have thermodynamically modeled a hybrid system for H$_2$ production and liquefaction. They aimed to provide a clean method for hydrogen production and liquefaction. Simulation was performed by the Aspen Plus software. The results obtained showed that the exergy and energy efficiencies of the hybrid system were 31.35% and 18.6%, respectively. Boyaghchi *et al*. [42] have evaluated and optimized the exergetic, exergo-economic, and exergo-environmental aspects of a novel hydrogen liquefaction model. They proposed a pre-cooling system using the cascade ORC and ejector refrigeration cycles to reduce power consumption in the H$_2$ liquefaction system. The results obtained revealed that COP increased by 10%, and the environmental impact (EI) per exergy unit decreased by 0.0309 $/MJ.

Numerous studies have been recently performed on H$_2$ liquefaction in order to reduce energy consumption and supply the power of hydrogen liquefaction structure. The present research work economically evaluates a combined H$_2$ liquefaction unit using the LAC recovery and renewable energies under the climatic states of Yazd, Iran. Further details of the simulated hybrid structure are provided in the reference [5], which was designed by the authors of this paper. The main innovation of the present work is the economic analysis of the developed hybrid system.

2. Methodology

This work was conducted to examine a hybrid H$_2$ liquefaction system using the LAC recovery for pre-cooling as well as cascade refrigeration units with helium and hydrogen refrigerants for liquefaction. Moreover, the CHP, renewable solar energy, and PVC units were employed to supply the cycle power. Figure 1 illustrates the block flow diagram (BFD) of the developed hybrid

system. Figure 2 indicates the diagram of H_2
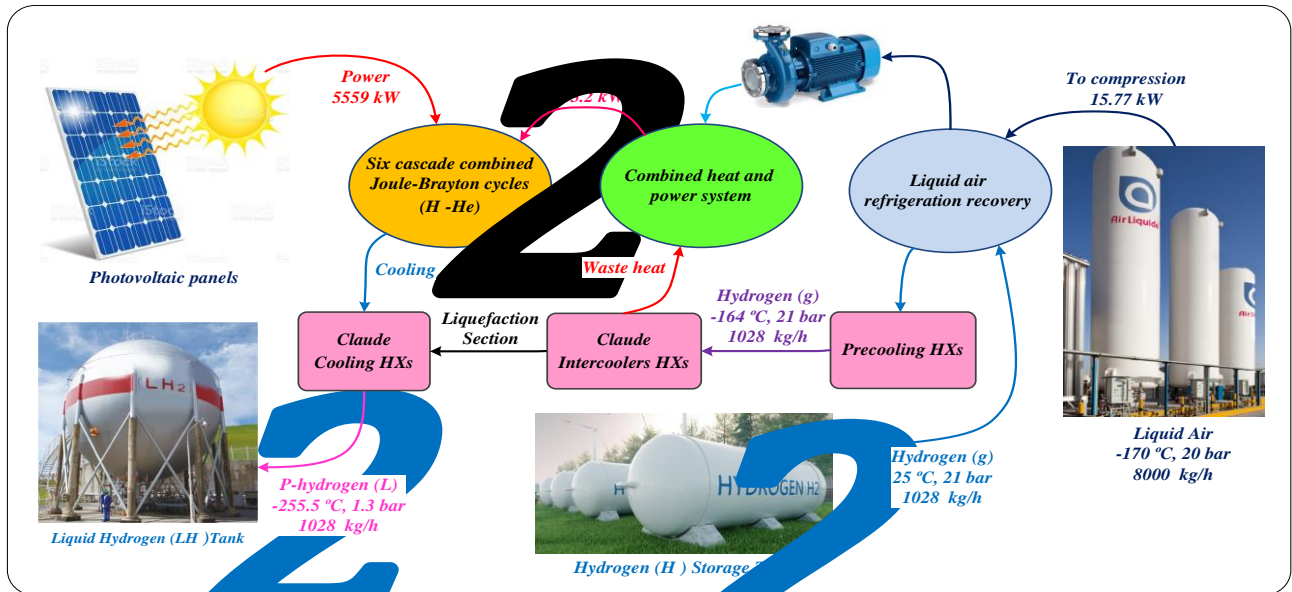
liquefaction process and its transport by ship.

Figure 1. Block flow diagram of the hybrid process (modified from Ref. [5]).
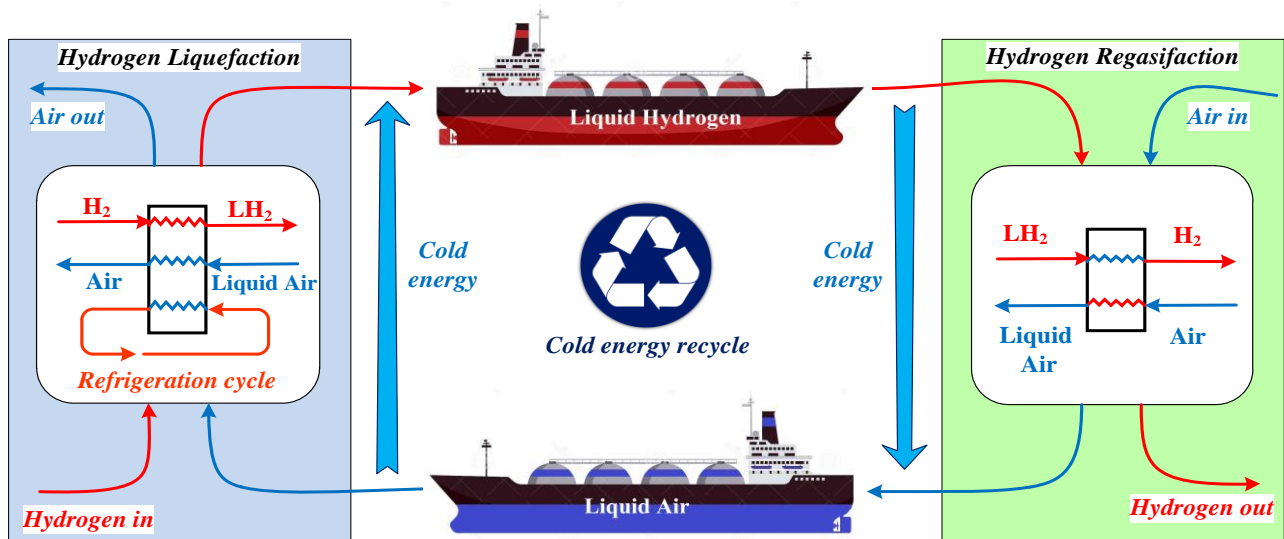

Figure 2. Diagram of H_2 liquefaction system and its transport by ship.

3. Process description

Given that hydrogen is a renewable and clean fuel with a high volume and pressure and low density, its application as a fuel in the storage and transportation processes poses challenges. Hence, hydrogen is stored as a gas. Hydrogen liquefaction is considered a suitable method, through which the problems of hydrogen transportation from origin to destination could be solved.

In this research work, a hybrid H_2 liquefaction structure was investigated using renewable energies and cold energy recovery of liquid air. The CHP and gas turbines were fed by the compressed liquid air passing through refrigeration recovery and reheating phases. The

hot outlet stream of CHP was used to supply the thermal energy of the power generation unit and pre-heat the inlet stream to CHP and gas turbine. The PVC units were used to supply the power of the hybrid H_2 liquefaction system under climatic conditions of Yazd. Further details of the simulated hybrid structure are provided in reference [5].

3.1. Hydrogen liquefaction cycle

Hydrogen molecules are present in the two ortho and para forms, which are in equilibrium under certain temperature conditions and play a major role in the hydrogen liquefaction cycle. Hydrogen includes 25% para and 75% ortho forms at the standard temperature and pressure. Catalytic

reactions are employed to accelerate ortho-para H_2 conversion in CR1 and CR2 conversion reactors. The ortho-para H_2 conversion is an involuntary and exothermic process. If ortho H_2 is not changed into para H_2 before being liquefied by a catalytic procedure, the heat produced by the ortho-para conversion causes most of the produced liquid H_2 to evaporate. Given that hydrogen tends to remain in the para form at temperatures below -193 °C, i.e. equilibrium temperature, the above conditions occur.

At the beginning of the hydrogen liquefaction cycle, stream H_1 with a temperature of 25 °C, pressure of 25 bar, and mass flow rate of 1028 kg/h enters the heat exchanger HE1 and its temperature reduces to -164 °C. The required refrigeration is provided by liquid air flow K2 to pre-cool the exchanger HE1. Then stream H_2 enters the exchanger HE5, and its temperature declines to -194.6 °C. The cascade refrigeration cycles with helium and H_2 refrigerants are used to cool the H_2 liquefaction cycle. Subsequently, stream H12 including para-H_2 with the temperature of -255 °C, pressure of 21 bar, and mass flow rate of 1028 kg/h enters the expander T7 and its pressure decreases by 1.3 bar. Then stream H13 leaves turbine T7 and enters flash drum D1. Finally, stream H15, which is the produced liquid H_2, exits from the bottom of flash drum D1. A part of the waste heat of H_2 liquefaction refrigeration system in heat exchangers HE10 and HE11 are employed to pre-heat the compressed air. In the gas turbines T8, T9, and T11, the compressed air enters SOFCs by reducing the pressure by stream H1 at the temperature of 30 °C, pressure of 1.34 bar, and mass flow rate of 2065 kg/h.

3.2. Solid oxide fuel cell

Fuel cells directly convert the chemical energy resulting from a reaction into useful electrical energy. Energy conversion efficiency of this system is very high so that its waste is very low or zero depending on the type of consumed fuel. Hydrogen fuel cells do not emit any pollution, and their only by-product is pure water vapor. Natural gas or other fuels are used to provide the required fuel for SOFCs. The overall fuel reforming reaction and water vapor is presented as equation 1 [7]:

$$CH_4 + 2H_2O \rightarrow 4H_2 + CO_2 \qquad (1)$$

In SOFCs, oxygen ion (O^{2-}) carries the charge and the electron is produced through the reaction of H_2 with the electrolyte transferred to the anode. In the heat exchanger HE20, a part of the outlet stream

from reactor R101, known as return stream K29, is used to pre-heat the input stream to the anode. The rest of the hot outlet stream goes to heat exchanger HE28 in the power production unit, and the temperature of stream S6 increases to 680 °C. Stream S6 has a high temperature and pressure but its pressure declines to 23.86 bar after entering turbine T10. Stream S7, which is the outlet current from gas turbine T10, goes to the compressors to increase the pressure and provide pre-heating.

3.3. PVC unit simulation

The international energy agency (IEA) has provided the necessary performance parameters to analyze the performance of on-grid PV systems. The final system yield, performance ratio, reference yield, inverter efficiency, array capture losses, system's total energy loss, array yield, etc. are among the parameters used for the feasibility analysis of the PVC power plants.

In this work, these parameters were used to evaluate the performance of the on-grid PVC system. The amount of on-grid energy was calculated on a daily, monthly or annual basis. Y_F represents the final system yield. The parameters employed in the PV system calculations are equal to the amount of final AC energy generated by the PVC system divided by the maximum power of the system under STC. The final yield of the system is obtained as follows [43]:

$$Y_F = \frac{E_{AC}}{P_{PV}} \qquad (2)$$

where Y_F is the final yield of the system (kWh/kWp), P_{PV} is the maximum output power of the system under STC, and E_{AC} is the amount of AC energy generated by the inverter (kWh). The nominal yield, known as reference yield, is assessed based on the total amount of energy generated by the system. The nominal yield of the systems could be observed in their datasheets, which are pre-determined by the manufacturers under STC.

The reference yield, Y_R, is presented in equation 3. Mathematically, this is the ratio of total in-plane solar radiation to global array reference irradiance under STC [43]:

$$Y_R = \frac{H_t(kWh/m^2)}{G_o(kW/m^2)} \qquad (3)$$

Y_A is the array yield, which is obtained by dividing the amount of DC energy generated by PV arrays (kWh) by the rated power of the PV array (kWp) under STC as follows [43]:

130

$$Y_A = \frac{E_{DC}}{P_O} \qquad (4)$$

PR is the performance ratio, which is obtained by dividing the final system yield by reference yield as follows [43]:

$$PR = Y_F / Y_R \qquad (5)$$

The system's total energy loss can be calculated as follows [43]:

$$L = Y_R - Y_F \qquad (6)$$

Array losses are expressed as the difference between the reference yield and array yield [43]:

$$L_C = Y_R - Y_A \qquad (7)$$

3.3.1. Inverter efficiency
The PV inverter efficiency can be calculated by equation 8, which is equal to the ratio of the inverter's AC power to DC power generated by the PV array [44]:

$$\eta_{inv} = \frac{P_{AC}}{P_{DC}} \qquad (8)$$

3.3.2. System efficiency
The PV system efficiency can be calculated by multiplying the module efficiency by the inverter efficiency as follows [45]:

$$\eta_{system} = \eta_{PV} \times \eta_{inv} \qquad (9)$$

In this work, the PVsyst 6.8.1 software was used to model the power generated by solar energy in PV panels.

3.4. Economic analysis
The low-temperature processes are among the energy-intensive processing industries due to the high costs of equipment and energy consumption. A major part of the initial and operating investment costs in these industries is related to the refrigeration cycle investment costs. The annualized cost of configuration (ACC) is selected to perform the economic analysis. The parameters of period of return, prime cost, and capital cost are among the important parameters for selecting an appropriate integrated hydrogen liquefaction structure.

3.4.1. Economic analysis of ACC
In this method, all costs of a structure within its estimated technical life are computed including the annualized capital price (C_{acap}), replacement price (C_{arep}), maintenance price (C_{amain}), and operating price (C_{aope}).
Given that the useful life of the project was assumed to be 20 years, C_{arep} was excluded. Eqs. (10) and (11) present the economic research of the

device of the hybrid structures. Some of the equations were related to the prior years. Thus they were updated using the Marshall and Swift price index.

$$Cost_{reference\ year} = Cost_{original\ year} \frac{Cost\ index_{reference\ cost\ year}}{Cost\ index_{original\ cost\ year}} \qquad (10)$$

The configuration of the integrated structures is obtained as follows:

$$ACS = C_{acap}(Components) + C_{arep}(Components) + C_{amain}(Components) +$$
$$C_{aope}(Labor\ Cost + Fuel\ Cost + Insurance\ Cost) \qquad (11)$$

3.4.2. Annualized capital cost (C_{acap})
C_{acap} includes costs of purchasing the above equipment, which are leveled throughout the useful life of each integrated structure. C_{acap} is obtained as follows:

$$C_{acap} = C_{Cap}.CRF(i, Y_{proj}) = C_{Cap}.\frac{i.(1+i)^{Y_{proj}}}{(1+i)^{Y_{proj}} - 1} \qquad (12)$$

in which C_{cap} is the total price of the device purchased, i is the real bank interest rate, Y_{proj} is the helpful life of the project, and CRF is the capital recovery factor. The annual inflation rate, f, and nominal interest rate, j, are used to compute the real bank interest rate as follows:

$$i = \frac{j-f}{1+f} \qquad (13)$$

For performing the economic research of the hybrid system, the annual inflation rate, nominal interest rate, and useful life of the system were supposed to be 17%, 20%, and 20 years, respectively.

3.4.3. Annualized operating cost (C_{aope})
C_{aope} includes the manpower, fuel consumption, and equipment insurance costs. In this work, the manpower cost was considered US$ 400 per person per month, and the equipment insurance cost was equal to 2% of the cost of purchasing them annually. The number of employees based on the reference size was considered 50. Moreover, the base price of natural gas, world market price of hydrogen based on natural gas reforming, and world market price of hydrogen were 1.8 US$/MMBTU, 2.5 US$/kg, and 7 US$/kg LH$_2$, respectively. It should be noted that these prices in the world markets vary depending on the temperature, pressure, composition, and product state.

3.4.4. Annualized maintenance cost (C_{amain})
In this work, C_{amain} of equipment used in

integrated structures in supercooled natural gas processes was considered 5% on average based on the useful life of the system. C_{amain} includes the costs of periodic maintenance and replacement of sensitive parts.

3.4.5. Calculating net present value (NPV)
By calculating NPV, all costs and revenues over the useful life of the integrated structures are converted into the current time or start time of the project. The total cost of the project in the beginning year can be obtained as follows:

$$NPV = \frac{ACS}{CRF(i,Y_{proj})} = ACS \cdot \frac{(1+i)^{Y_{proj}}-1}{i.(1+i)^{Y_{proj}}} \qquad (14)$$

3.4.6. Levelized cost of product (LCOP)
LCOP is equal to the average cost incurred per unit of production over the useful life of the project. LCOP is obtained by equation 15, and it is an appropriate criterion for comparing integrated structures from an economic issue of view:

$$LCOP = \frac{ACS}{Annual\ output\ product\ of\ the\ system} \qquad (15)$$

The market price of a product is equal to the prime cost plus the normal profit that the producer adds to the prime cost. Therefore, LCOP is a suitable criterion for comparing two or more systems from an economic viewpoint but it is not a good criterion for comparing the market price of a product. A new parameter, called prime cost (PC), is defined to select an appropriate criterion for comparing the product price and market price of the product.

3.4.7. Prime cost of product (PC)
The capital cost (CC), operating flow cost (OFC), and annual volume of product (VOP) should be examined to calculate PC. CC includes the costs of purchasing equipment and installing the system. The installation cost is equal to 10% of the total cost of purchasing the equipment. OFC includes the fuel, manpower, maintenance, and equipment insurance costs on an annual basis, each of which is separately assessed. The annual VOP calculates the total production volume per year.
In this work, considering the times when the system is out of circuit for reasons such as network outage and system maintenance, the number of hours that the system was ready to operate was considered 85% of the total hours of

the year (7,446 hours).
PC can be obtained by equation 16. Cost of product (COP) denotes the product price in the market.

$$PC = \frac{OFC}{VOP} \qquad (16)$$

The summary of product cost (SOPC) is defined as the total revenue obtained from selling the product in the market, which can be calculated by equation 17.

$$SOPC = (VOP) \times (COP) \qquad (17)$$

3.4.8. Gross annual benefit (AB)
Gross annual benefit (AB) is the difference between the system's OPC and total revenue obtained from selling the manufactured products in the market (equation 18). The revenue from selling ancillary products, just like the revenue from selling the main product, is added to the gross benefit.

$$AB = SOPC - OFC \qquad (18)$$

3.4.9. Net annual benefit (NAB)
NAB is obtained by subtracting the tax from the total calculated income (equation 19). The VAT rate was considered 10%.

$$NAB = AB \times (1 - Tax\ Percent)$$
$$Tax = 0.1 \times AB \qquad (19)$$

3.4.10. Key parameters of economic analysis
The three parameters of return (POR), rate of return (ROR), and additive value (AV) are the essential parameters of economic analysis (Eqs. 20-22).

$$POR = \frac{CC}{NAB} \qquad (20)$$

$$ROR = \frac{NAB}{CC} \qquad (21)$$

$$AV = COP - PC \qquad (22)$$

AV refers to the difference between the prime cost of a product and its sale rate in the market thath can accept various values relying on how advanced the technology employed in the generation process is. Table 1 illustrates the equations utilized to calculate the equipment cost of the integrated structures.
Table 2 shows the economic study of the integrated hydrogen liquefaction system using the LCA. recovery and SOFCs.

Table 1. Equations utilized to calculate equipment costs of the hybrid process structures.

Component	Purchased equipment cost functions
Compressor	$C_{Com} = \left(\dfrac{39.5 \times \dot{m}}{\eta_C}\right)\left(\dfrac{p_{discharge}}{p_{suction}}\right) \ln\left(\dfrac{p_{discharge}}{p_{suction}}\right)$ C_{Com} = Cost of compressor (k$)
Photovoltaic	C_{PV}=840 \$/m^2 (PV array cost) $C_{Batery\ cost}$ =220 \$/kWh, $C_{Inverter\ cost}$ =750 \$/kWh $C_{Diesel\ genset\ cost}$ =550 \$/kWh
Heat exchanger	$C_E = a(V)^b + c$ C_E = Cost of heat exchanger (\$)
Condenser	$C_C = 516.6 \times A_{Condenser} + 268.4$
Pump	$C_p = 705.4 \times W_{Pump}^{0.71}\left(1 + \dfrac{0.2}{1\text{-}\eta_{Pump}}\right)$
Burner	$C_{Burner} = \left(\dfrac{46.08 \times \dot{m}_{in}}{0.995 - \left(\dfrac{P_{out}}{P_{in}}\right)}\right)(1 + \exp(0.018 T_{Burner} - 26.4))$
Turbine	$\text{Cost}_{Ex} = 0.378(\dot{W}\ \text{(horsepower)})^{0.81}$
SOFC	$C_{SOFC} = 2000(\dot{W}\ \text{(kW)})$
General heat exchanger	$C_{HX} = 8500 + 409 \times A_{HX}^{0.85}$
Flash drum	$C_D = f_m C_b + C_a$ C_D = Cost of drum (\$) $C_b = 1.218\exp[9.1 - 0.2889(lnW) + 0.04576(lnW)^2]$, 5000<W<226000 lb shell weight $C_a = 300 D^{0.7396} L^{0.7066}$, 6<D<10, 12<L<20 ft f_m = Material Factor

Table 2. Economic analysis of integrated H$_2$ liquefaction cycle by LCA recovery and renewable energies.

Definition	Parameter
Annualized cost of system	*ACC=Cacap (Components) + Carep (Components) + Camain (Components) + Caope (Labor Cost+ Fuel Cost+ Insurance Cost)*
Annualized capital cost	*Ccap= 1.1 of Total capital cost* $Cacap = Ccap.CRF(i,Yproj) = Ccap.\dfrac{i.(1+i)^{Y_{proj}}}{(1+i)^{Y_{proj}} - 1}$ $i = \dfrac{j - f}{1 - f}$
Annualized replacement cost	$Crap = Ccap(\text{In Base}).(1+i)^{Y_{proj}}$ $Carep = Crap.SFF(I,Yproj) = Crap.\dfrac{j}{(1+i)^{Y_{proj}} - 1}$
Annualized maintenance cost	*For Yproj=20 , Camain=0.05 of Capital Cost*
Annualized operating cost	*OFC= (Labor Cost+ Fuel Cost+ Insurance Cost+ Utility)* *Number of labor = 50 , Labor Cost =400 US$ per Month* *Fuel Cost (Natural Gas Price)= 1.8 (US$ per Million Btu)*
Operating flow cost	*Fuel Cost (Hydrogen Gas Price)= 2.5 (US$ per kg H$_2$)* *Insurance Cost=0.02 of Capital Cost*
Net present value	*NPV= ACC/ CRF(i,Yproj)*
Levelized cost of product Total product in one year (kg LNG)	*LCOP= ACC/ Total Product in one Year*
Prime cost	*VOP= Volume of Product , PC=OFC/VOP*
Summary Of product cost	*COP= Cost Of Product, SOPC= VOP. COP* *COP=7 (US$ per kg H$_2$)*
Annual benefit	*AB= SOPC- OFC*
Net annual benefit	*NAB= AB.(1-Tax percent) , Tax=0.1(AB)*
Period of return	*POR= Ccap/NAB*
Rate of return	*ROR= NAB/ Ccap*
Additive value	*AV=COP-PC*

4. Discussion and results

4.1. PV system simulation results
Given that Yazd is geographically located at the longitude of 54° 21' E and latitude of 31° 53' N and is 1,226 m above the sea level, the PV system modeling was performed. The total power required for developing the integrated cycle was determined as 5,559 kW based on the information contained in the simulated cycle in the ASPEN HYSYS V10 software. Table 3 presents the specifications of the studied PVC system.

Figure 3 compares the monthly yield and energy production of the reference (Afrouzy *et al*., 2021) and proposed models.

Table 3. Specifications of studied PVC system.

Specification		
Electrical performance under standard test conditions (*STC)		
Highest power (Pmax)	400 W (±%3)	
Highest power voltage (Vmpp)	649 V	
Highest power current (Impp)	7960 A	
Open circuit voltage (Voc)	955 V	
Short circuit voltage (Isc)	8368 A	
Highest system voltage	1000 V	
Temperature coefficient of Voc	-142 mV/°C	
Temperature coefficient of Isc	3.1 mA/°C	
*STC: irradiance 1000 W/m², module temperature 25°C		

Electrical performance at 1000 W/m², NOCT	
Highest power (Pmax)	402.3 W
Highest power voltage (Vmpp)	41.3 V
Highest power current (Impp)	9.74 A
Open circuit voltage (Voc)	50.5 V
Short circuit voltage (Isc)	10.23 A
Nominal operating cell temperature (NOCT): 25 °C	

Cell	
Number per module	72

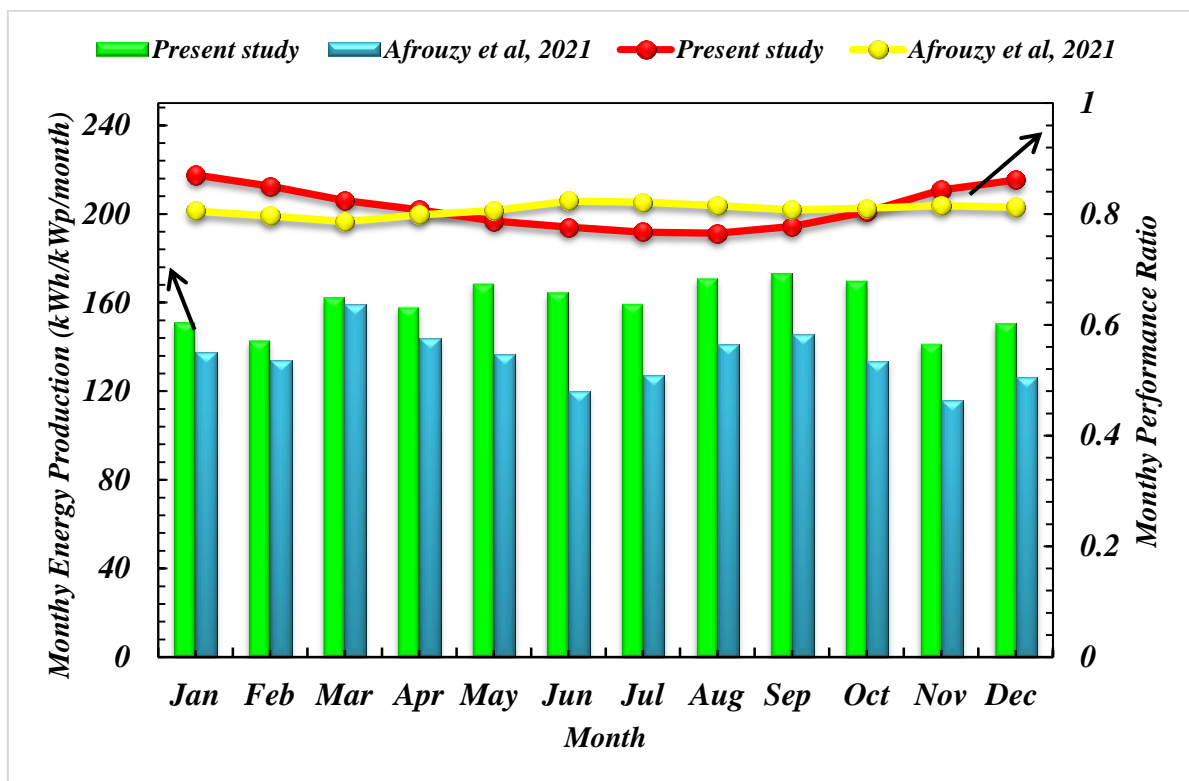| Module characteristics	
Length × Width × depth (mm)	2064 × 1024 × 40
Weight (kg)	22
Manufacturer	LG Electronics
Description and details	LG 400 N2T-A5

Figure 3. Comparing monthly yield and energy production of the reference (Afrouzy *et al*., 2021) and proposed models.

The geographical characteristics and meteorological data of the desired location should be thoroughly examined to model the PVC unit and supply the required energy of the structure. In this work, the fixed-tilt panels were used for the designed model, the monthly average horizontal solar irradiation of which was at the angle of 32°. This angle was regarded as the slope angle of PVC units. Figure 4 indicates the monthly average environmental temperature and solar irradiation in a typical year in Yazd.
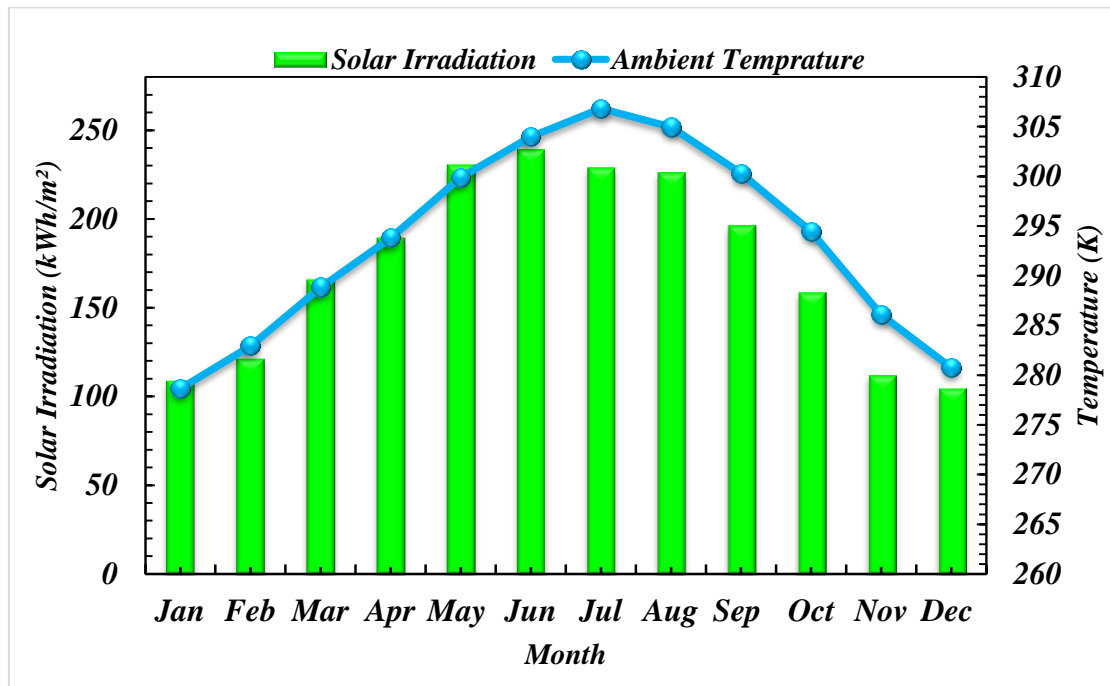
134

Figure 4. Monthly average ambient temperature and solar irradiation in a typical year in Yazd.

As demonstrated in figure 4, the monthly average horizontal global radiation in Yazd ranges from 104.8 kWh/m² in December to 239.0 kWh/m² in June. Moreover, July is the hottest month of the year with the monthly average temperature of 306.8 K, and January is the coldest month of the year with the temperature of 278.6 K. The average environmental temperature in a typical year is 293.5 K in Yazd. Figure 5 depicts the performance ratio (PR), array outcome energy, and energy injected into the grid.
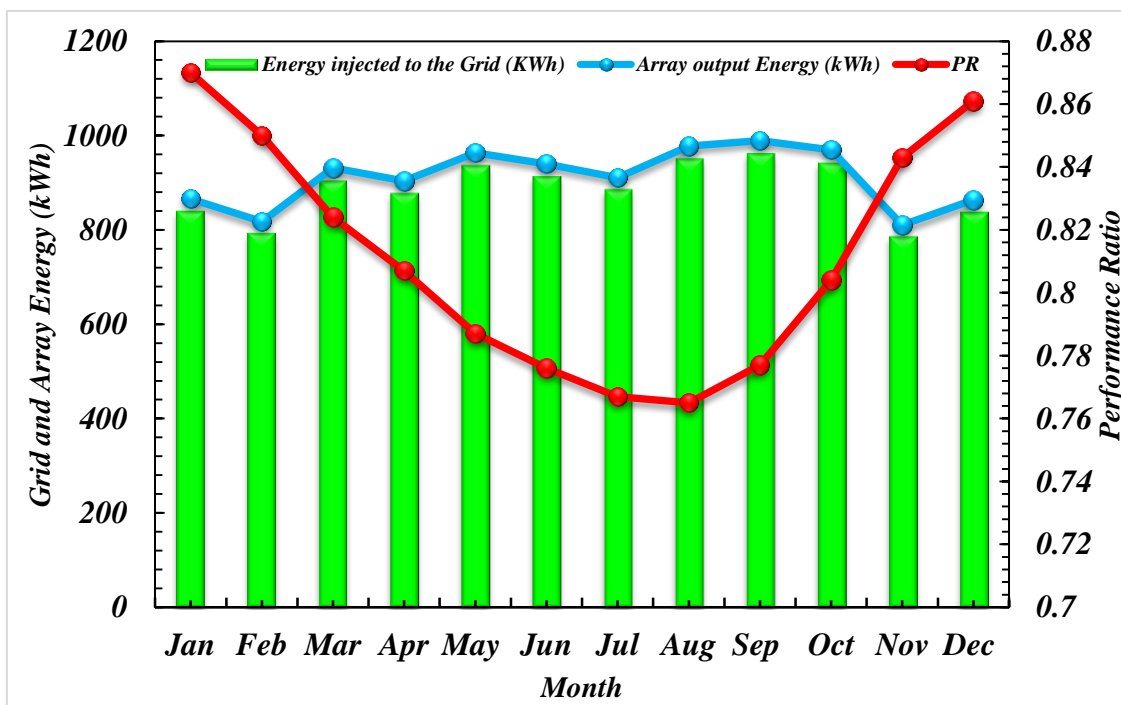

Figure 5. Monthly array energy production and energy injected into grid and PR.

Figure 5 illustrates the monthly solar energy injection in different systems during the year. The highest and lowest PRs were in January (87%) and August (76.5%), respectively. The annual mean value of PR was specified as 80.8%. The highest and lowest available energy were showed in September (962.2 kWh) and November (786.7 kWh), respectively, which could be due to the

135

relatively higher global solar irradiance on tilted planes in various months of the year. Figure 6 illustrates the PVC unit and collection losses as well as useful energy production.
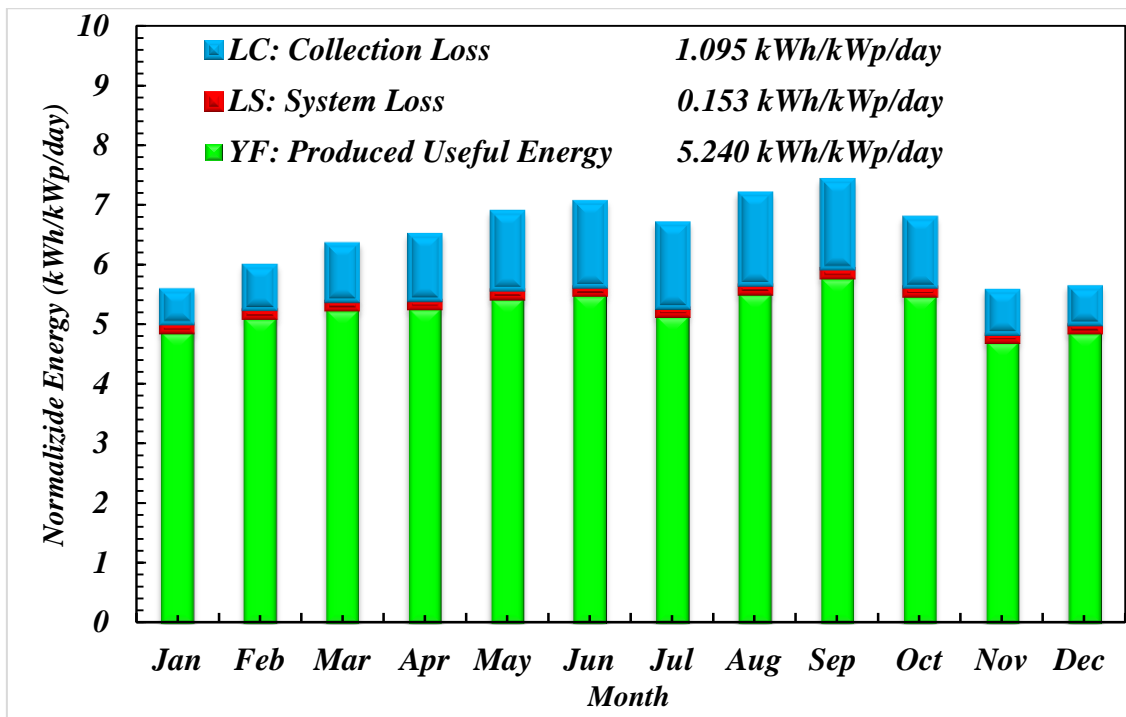

Figure 6. Normalized energy per month.

Solar energy is absorbed by the PVC panels. Thus this energy decreases due to collection losses during absorption, and is distributed to the inverters. The distributed energy is injected into the grid as the useful energy. Figure 8 indicates the system, array, and inverter efficiencies in a typical year in Yazd.
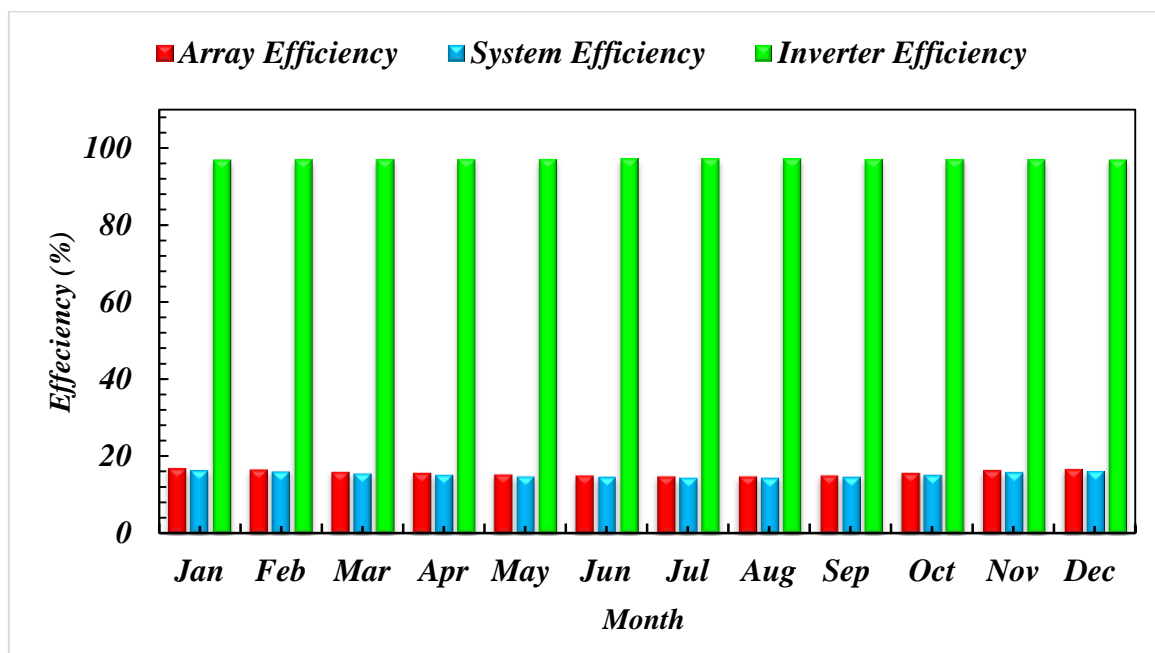

Figure 7. System, array, and inverter efficiencies in a typical year in Yazd.

The PVC panels can generate electricity in a wide range of optical frequencies. However, since they are not able to cover the entire spectrum of the sunlight, a great amount of solar energy is wasted. Figure 8 indicates the PVC system losses during the year based on simulations.
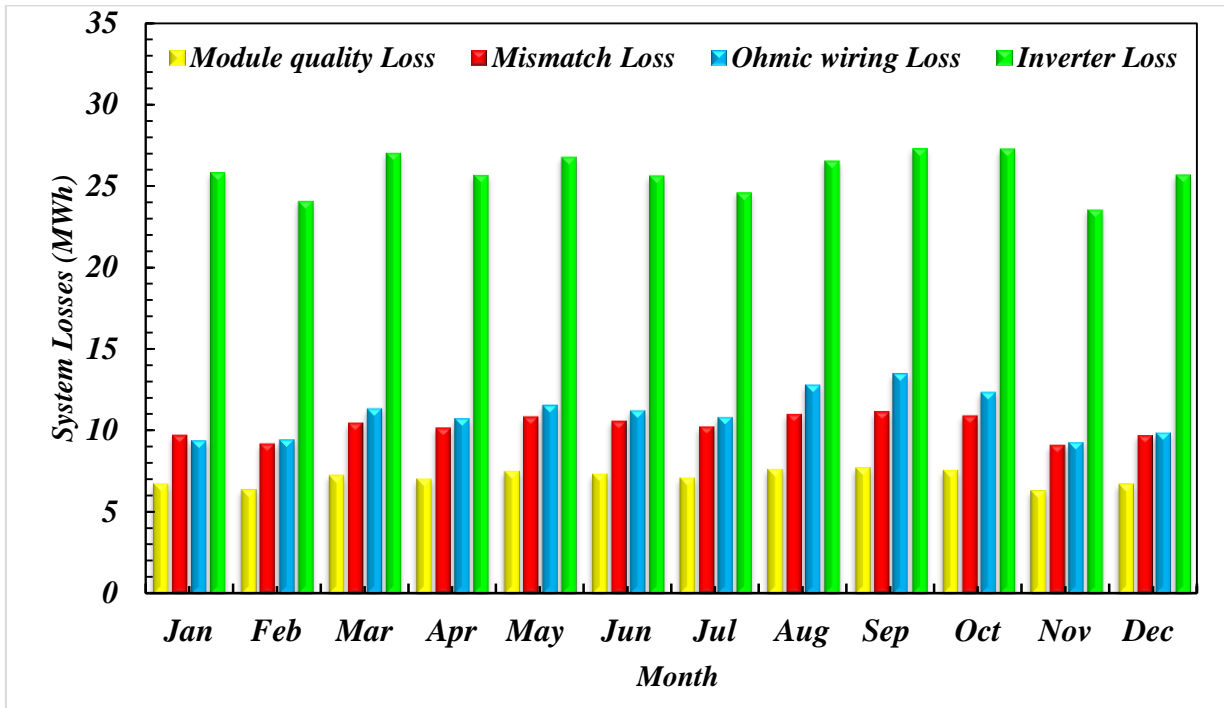
Figure 8. Diagram of system losses over the whole year in Yazd.

The modeling results revealed that selecting an improper cable size and length could directly affect ohmic wiring loss, the mean annual value of which was 132.4 MWh. The mean annual value of module quality loss was 85.06 MWh. The highest and lowest values of mismatch loss were in September (7.704 MWh) and November (6.295 MWh), respectively.

4.2. Economic analysis results

In this work, feasibility of the integrated structure and the ACC method was evaluated in order to perform the economic analysis. Figures 9-14 present the analysis results.

Figure 9 indicates the impact of gaseous hydrogen cost on the prime cost of liquid hydrogen and net annual benefit gained from sales. The net annual benefit decreases to 5.366 MMUSD/Year, and the prime price of the product increases up to 6.947 USD/kg LH_2, respectively, with the increase of hydrogen gas price from 1.4 to 3.4 USD/kg H_2 .
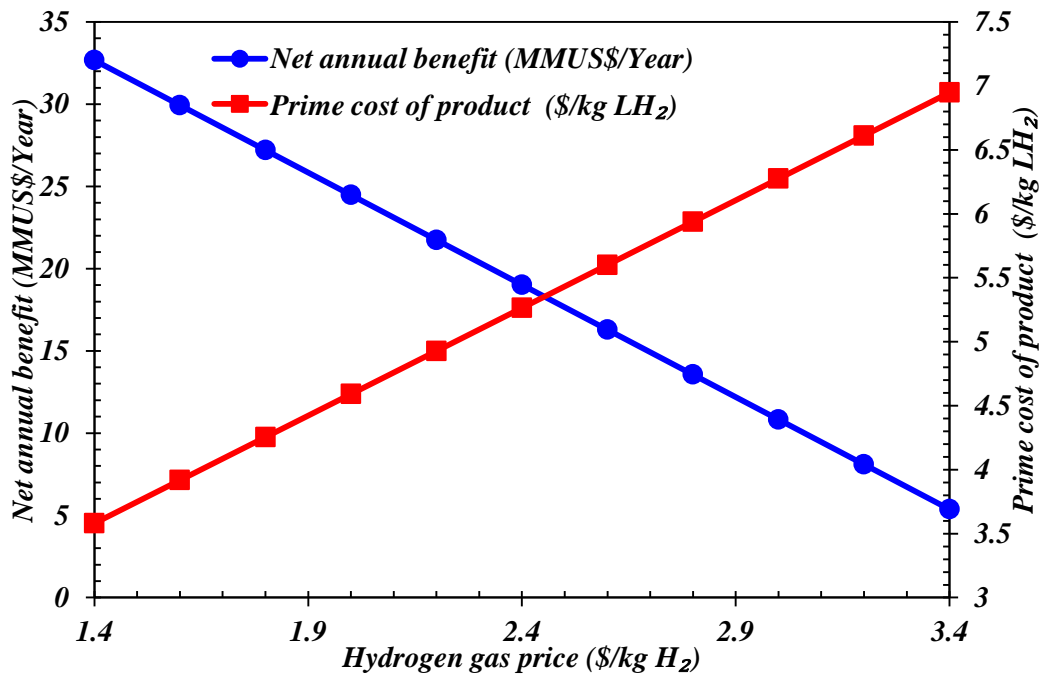

Figure 9. Impact of gaseous hydrogen cost on prime cost of liquid hydrogen and net annual benefit gained from sales.

Figure 10 indicates the impact of gaseous hydrogen cost on the annualized operating cost of the system and levelized cost of product. The levelized cost of product and annualized operating cost increase up to 6.875 USD/kg LH_2 and 57.09 MMUSD/kg LH_2, respectively, with the growth of hydrogen gas price from 1.4 to 3.4 USD/kg H_2 .
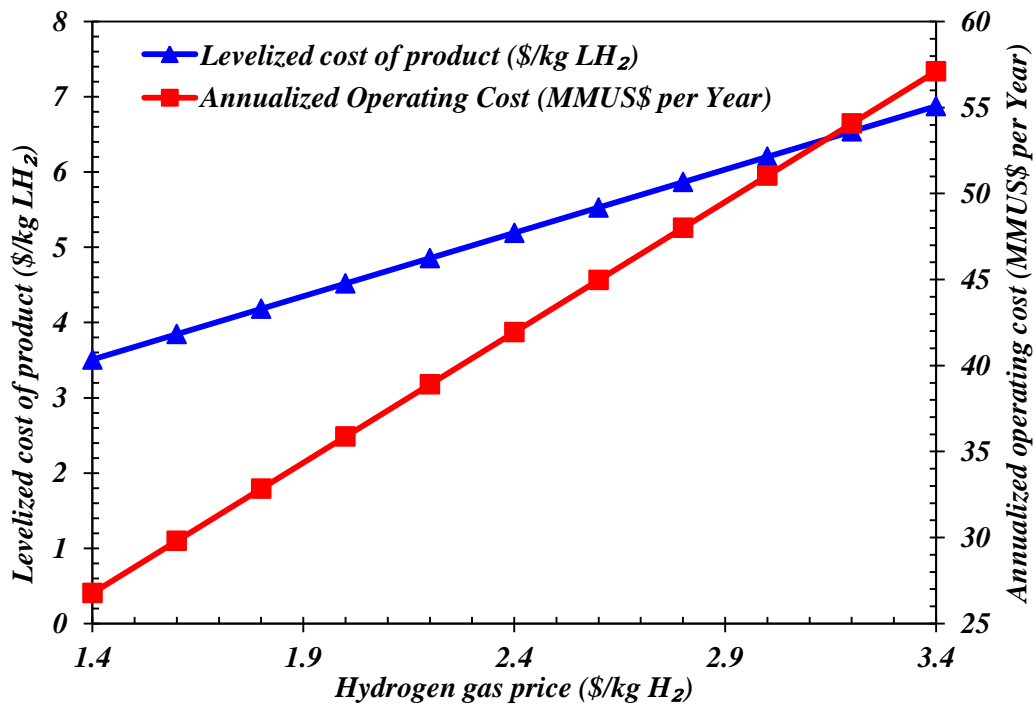

Figure 10. Impact of gaseous hydrogen cost on annualized operating cost of system and levelized cost of product.

Figure 11 indicates the impact of gaseous hydrogen cost on POR of the integrated structure and AV of the product. The additive value decreases to 0.0524 USD/kg LH_2, and the period of return increases up to 13.97 years, respectively, with the increase of hydrogen gas price from 1.4 to 3.4 USD/kg H_2 .
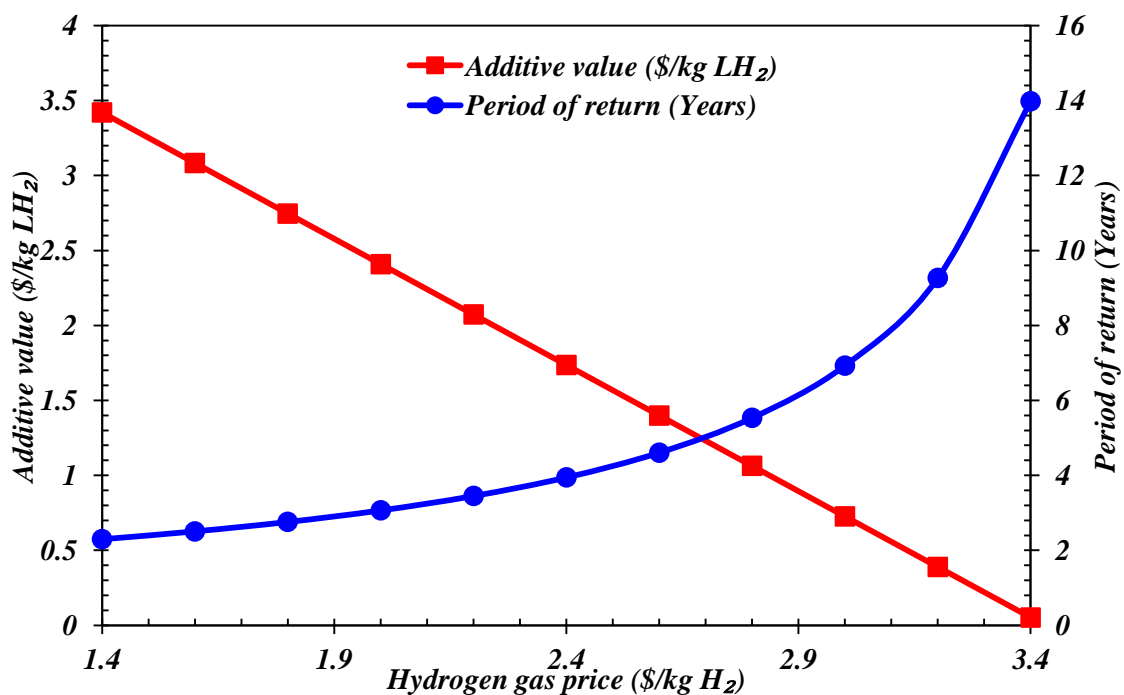

Figure 11. Impact of gaseous hydrogen cost on POR of integrated structure and AV of product.

Figure 12 indicates the impact of capital cost on POR of the integrated structure and AV of the product. The additive value decreases to -0.6468 USD/kg LH_2, and the period of return increases up to 25.07 years, respectively, with the increase of capital cost price from 52.5 to 217.5 MMUSD.
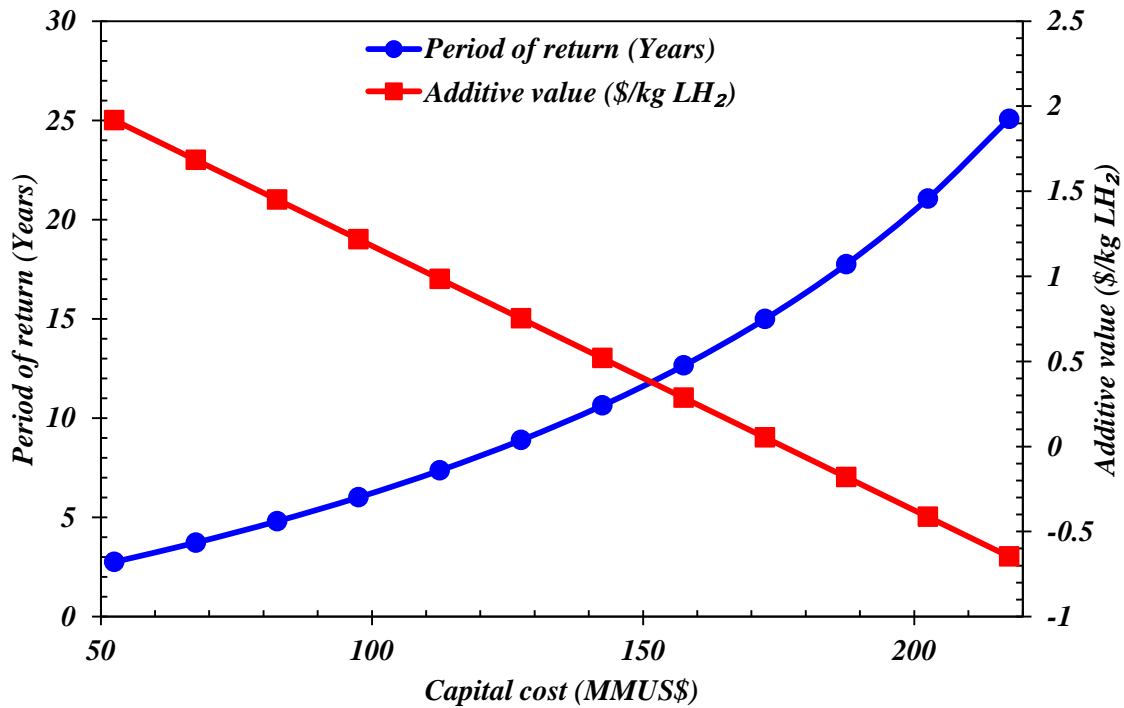

Figure 12. Impact of capital cost on POR of e integrated structure and AV of product.

Figure 13 indicates the effect of capital cost on the prime cost of liquid hydrogen and net annual benefit gained from sales. The Net annual benefit decreases to 8.673 MMUSD/Year, and the prime cost of product increases up to 7.646 USD/kg LH_2 years, respectively, with the increase of capital cost price from 52.5 to 217.5 MMUSD.
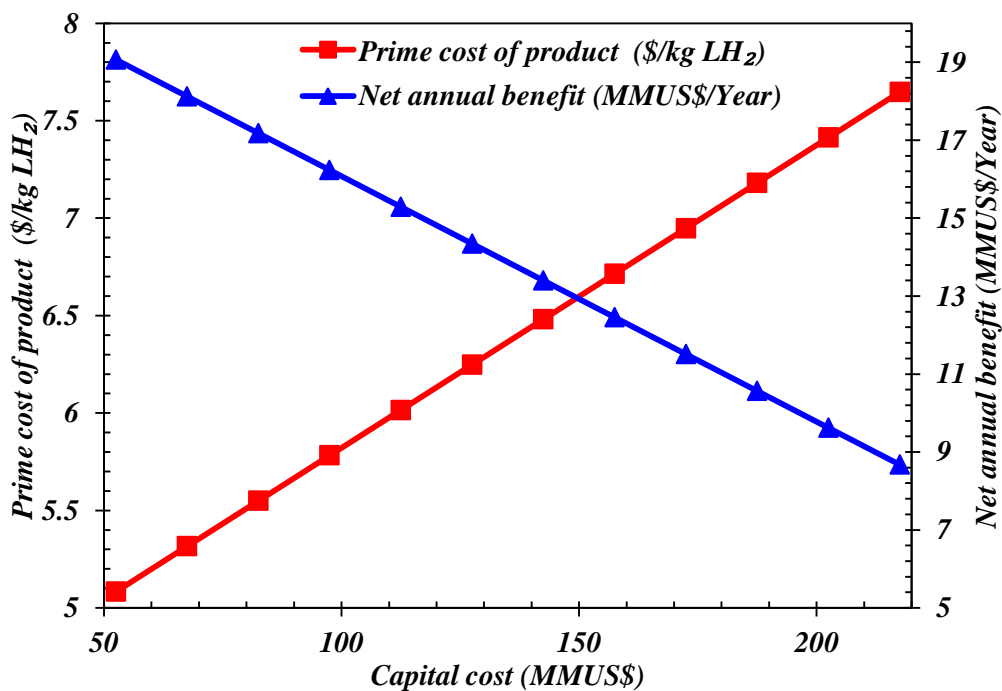

Figure 13. Effect of capital price on prime cost of liquid hydrogen and net annual benefit gained from sales.

Figure 14 indicates the impact of capital cost on the annualized operating cost of the system and levelized cost of product. The levelized cost of product and annualized operating cost increase up to 7.488 USD/kg LH_2 and 53.42 MMUSD/kg LH_2, respectively, with the growth of capital cost price from 52.5 to 217.5 MMUSD.
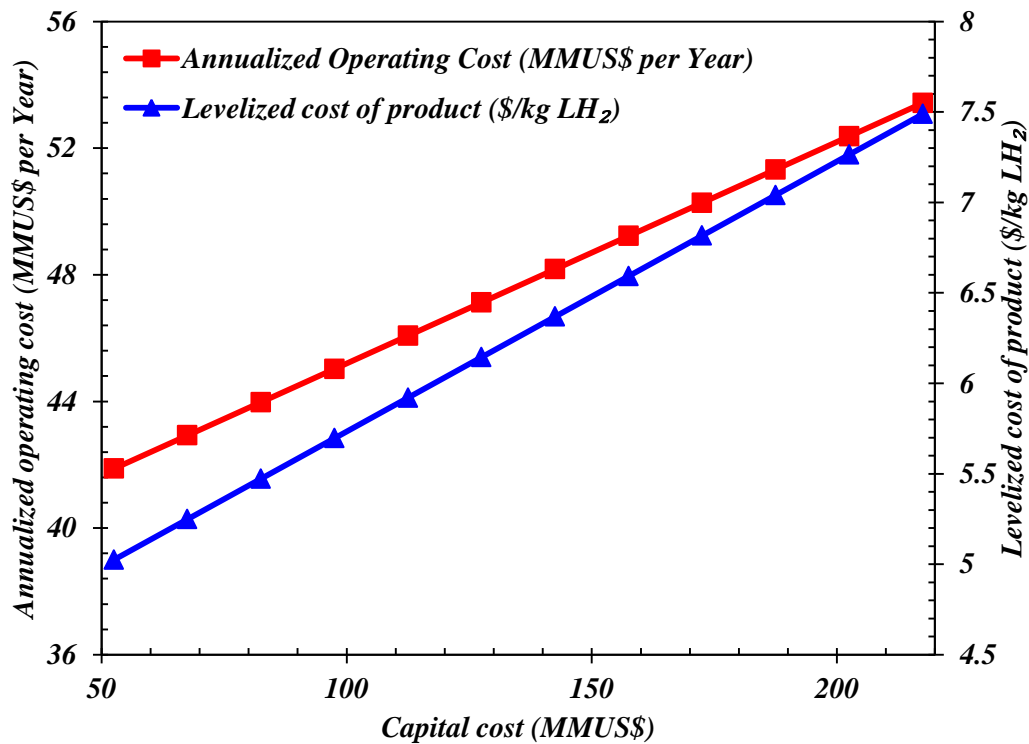

Figure 14. Impact of capital cost on annualized operating cost of system and levelized cost of product.

5. Conclusion

The low-temperature liquefaction systems could be used for long-term hydrogen storage and transport to distant places. The low-temperature systems include the reactors, heat exchanger networks, and refrigeration systems, which are completely interdependent. The complicated relations between these sections have made the design of the combined low-temperature systems always one of the most challenging problems in hydrogen liquefaction cycles. The low-temperature hydrogen liquefaction units are between the energy-intensive processing industries owing to the high prices of device and energy consumption. A significant section of the initial and operating capital prices in the low-temperature systems is related to the low-temperature refrigeration system prices. Therefore, the economic analysis of integrated hydrogen liquefaction systems is of particular importance in order to assess their feasibility.

In this research work, the combined hydrogen liquefaction systems were economically evaluated by the ACC method. Moreover, the LAC recovery and cascade refrigeration units with helium and hydrogen refrigerants were utilized for pre-cooling and H_2 liquefaction. The waste heat of fuel cells was applied in the power production unit to pre-cool the inlet streams to fuel cells. The developed hybrid system generated 1028 kg/h of liquid H_2 under climatic conditions of Yazd by receiving 5559 kW of power from PVC unit, 60.79 kg/h of natural gas and 1028 kg/h of gaseous H_2. SPC of the H_2 liquefaction cycle as well as the SOFC and power generation cycle efficiencies were calculated as 5.95 kWh/kg LH_2, 0.629, and 0.604, respectively.

Analyzing the economic sensitivity of hydrogen liquefaction systems revealed the period of return increased from 2.295 to 13.97 years, and additive value decreased from 3.419 to 0.0524 USD/kg H_2 by increasing the gaseous hydrogen cost from 1.4 to 3.4 USD/kg H_2. The annualized operating cost and levelized cost of product increased to 57.09 MMUSD/year and 6.875 USD/kg LH_2, respectively. POR increased from 2.753 to 25.07 years, and the net annual benefit decreased from 19.06 to 8.673 MMUSD/year by increasing the capital cost from 52.5 to 217.5 MMUSD. The annualized operating cost and levelized cost of product increased to 53.42 MMUSD/year and 7.488 USD/kg LH_2, respectively.

It is recommended to perform further studies on the risk analysis and operational optimization of

multi-component refrigerant composition using the meta-heuristic optimization algorithms.

6. Nomenclature

Abbreviations	
SEC	Specific energy consumption
PV	Photovoltaic
SOFC	Solid oxide fuel cell
POR	Period of return
AV	Additive value
CO_2	Carbon dioxide
RTE	Round-trip efficiency
MCFC	Molten carbonate fuel cell
CORC	Cascade organic Rankine cycle
HTES	High-temperature thermal energy storage
GT	Gas turbine
MR	Mixed refrigerant
PEM	Polymer electrolyte membrane
PV	Photovoltaic
TEACS	Triple-effect absorption cooling system
LNG	Liquefied natural gas
LAES	Liquid air energy storage
RTE	Round-trip efficiency
EI	Environmental impact
BFD	Block flow diagram
PFD	Process flow diagram
IEA	The international energy agency
ACC	Annualized cost of configuration
C_{acap}	Annualized capital cost
C_{arep}	Annualized replacement cost
C_{amain}	Annualized maintenance cost
C_{aope}	Annualized operating cost
NPV	Net present value
LCOP	Levelized cost of product
PC	Prime cost
CC	Capital cost
OFC	Operating flow cost
VOP	Annual volume of product
COP	Cost of product
SOPC	Summary of product cost
AB	Annual benefit
NAB	Net annual benefit
POR	Parameters of return
ROR	Rate of return
Pmax	Maximum power
Vmpp	Maximum power voltage
Impp	Maximum power current
Voc	Open circuit voltage
Isc	Short circuit voltage
STC	Standard test conditions
NOCT	Nominal operating cell temperature
SMR	Steam-methane reforming
CHP	Combined heating, and power
H_2	Hydrogen
Greek Letters	
Σ	Sum
η	Efficiency
η_{ohmic}	Voltage drop due to ionic and electronic conductivity of the electrolyte
$\eta_{act,c}$	Voltage drop due to cathode activation
$\eta_{conc,a}$	Voltage drop due to anode mass transfer
$\eta_{conc,c}$	Voltage drop due to cathode mass transfer
$\eta_{act,a}$	Voltage drop due to anode activation
Components Name	
HE	Heat exchanger
T	Turbine
R	Reactor
P	Pump
MIX	Mixer
X	Component splitter
G	Gibbs reactor
E	Equilibrium reactor
C	Compressor
D	Flash drum

7. References

[1] Wolfgang Lubitz and William Tumas, Hydrogen: An Overview, Chemical Reviews 107, 2007.

[2] "Liquefaction of hydrogen with emphasis on precooling processes." 12th Cryogenic - IIR Conference. Dresden. (2012).

[3] Notardonato, W. U., "Analysis and Testing of an Integrated Refrigeration and Storage System for Liquid Hydrogen Zero Boil-Off, Liquefaction, and Densification." (2006), University of Florida.

[4] Chanchetti, Lucas Faccioni, Daniel Rodrigo Leiva, Leandro Innocentini Lopes de Faria, and Tomaz Toshimi Ishikawa. "A scientometric review of research in hydrogen storage materials." International Journal of Hydrogen Energy 45(8), (2020): 5356-5366.

[5] Masoud Taghavi, Hesamoddin Salarian, and Bahram Ghorbani, "Thermodynamic and exergy evaluation of a novel integrated hydrogen liquefaction structure using liquid air cold energy recovery, solid oxide fuel cell and photovoltaic panels," Journal of Cleaner Production 320. (2021): 128821.

[6] L. El Chaar, L. A. lamont, and N. El Zein, Review of photovoltaic technologies, Renewable and Sustainable Energy Reviews 15(5), (2011), 2165-2175.

[7] Omar Z. Sharaf and Mehmet F. Orhan, An overview of fuel cell technology: Fundamentals and applications, Renewable and Sustainable Energy Reviews 32, (2014), 810-853.

[8] G. Squadrito, L. Andaloro, M. Ferraro, and V. Antonucci, Hydrogen fuel cell technology, Advances in Hydrogen Production, Storage and Distribution, (2014), 451-498.

[9] Ahmad Naquash, Muhammad Abdul Qyyum, Muhammad Islam, Noman Raza Sial, Seongwoong Min, Sanggyu Lee, and Moonyong Lee. "Performance enhancement of hydrogen liquefaction process via absorption refrigeration and organic Rankine cycle-

assisted liquid air energy system." Energy Conversion and Management 254 (2022): 115200.

[10] Amjad Riaz, Muhammad Abdul Qyyum, Seongwoong Min, Sanggyu Lee, Moonyong Lee. "Performance improvement potential of harnessing LNG regasification for hydrogen liquefaction process: Energy and exergy perspectives." Applied Energy 301 (2021): 117471.

[11] Øivind Wilhelmsen, David Berstad, Ailo Aasen, Petter Nekså, Geir Skaugen. "Reducing the exergy destruction in the cryogenic heat exchangers of hydrogen liquefaction processes." International Journal of Hydrogen Energy 43(10), (2018): 5033-5047.

[12] Mohammad Hossein Nabat, Mirhadi Zeynalian, Amir Reza Razmi, Ahmad Arabkoohsar, and M. Soltani. "Energy, exergy, and economic analyses of an innovative energy storage system; liquid air energy storage (LAES) combined with high-temperature thermal energy storage (HTES)." Energy Conversion and Management 226 (2020): 113486.

[13] Yunus Emre Yuksel, Murat Ozturk, Ibrahim Dincer. "Energy and exergy analyses of an integrated system using waste material gasification for hydrogen production and liquefaction." Energy Conversion and Management 185 (2019): 718-729.

[14] Ahmad Naquash, Muhammad Abdul Qyyum, Seongwoong Min, Sanggyu Lee, and Moonyong Lee. "Carbon-dioxide-precooled hydrogen liquefaction process: An innovative approach for performance enhancement–Energy, exergy, and economic perspectives." Energy Conversion and Management 251 (2022): 114947.

[15] Önder Kaşka, Ceyhun Yılmaz, Onur Bor, and Nehir Tokgöz. "The performance assessment of a combined organic Rankine-vapor compression refrigeration cycle aided hydrogen liquefaction." International Journal of Hydrogen Energy 43(44), (2018): 20192-20202.

[16] Jae-Hyeon Yang, Younggak Yoon, Mincheol Ryu, Su-Kyung An, Jisup Shin, and Chul-Jin Lee. "Integrated hydrogen liquefaction process with steam methane reforming by using liquefied natural gas cooling system." Applied Energy 255 (2019): 113840.

[17] Mohammad Hasan Khoshgoftar Manesh and Bahram Ghorbani. "Energy and exergy analyses of an innovative energy storage configuration using liquid air integrated with Linde-Hampson liquefaction system, molten carbonate fuel cell, and organic Rankine cycle." Journal of Energy Storage (2021): 103676.

[18] Murat Koc, Yunus Emre Yuksel, and Murat Ozturk. "Thermodynamic assessment of a novel multigenerational power system for liquid hydrogen production." International Journal of Hydrogen Energy (Available online 11 January 2022).

[19] Yujing Bi, Liang Yin, Tianbiao He, and Yonglin Ju. "Optimization and analysis of a novel hydrogen liquefaction process for circulating hydrogen refrigeration." International Journal of Hydrogen Energy 47(1), (2022): 348-364.

[20] Shengan Zhang, Guilian Liu. "Design and performance analysis of a hydrogen liquefaction process." Clean Technologies and Environmental Policy 24 (2022): 51-65.

[21] Saman Faramarzi, Seyed Mojtaba Mousavi Nainiyan, Mostafa Mafi, and Ramin Ghasemiasl. "A novel hydrogen liquefaction process based on LNG cold energy and mixed refrigerant cycle." International Journal of Refrigeration 131 (2021): 263-274.

[22] Armin Ebrahimi, Mohammad Hossein Monajati Saharkhiz, and Bahram Ghorbani. "Thermodynamic investigation of a novel hydrogen liquefaction process using thermo-electrochemical water splitting cycle and solar collectors." Energy Conversion and Management 242 (2021): 114318.

[23] Dongjun Lee, Dela Quarme Gbadago, Youngtak Jo, Gyuyoung Hwang, Yeonpyeong Jo, Robin Smith, and Sungwon Hwang. "Integrating hydrogen liquefaction with steam methane reforming and CO2 liquefaction processes using techno-economic perspectives." Energy Conversion and Management 245 (2021): 114620.

[24] Shaimaa Seyam, Ibrahim Dincer, and Martin Agelin-Chaab. "Analysis of a clean hydrogen liquefaction plant integrated with a geothermal system." Journal of Cleaner Production 243 (2020): 118562.

[25] Yunus Emre Yuksel, Murat Ozturk, and Ibrahim Dincer. "Analysis and assessment of a novel hydrogen liquefaction process." International Journal of Hydrogen Energy 42(16), (2017): 11429-11438.

[26] Anwar Hammad and Ibrahim Dincer. "Analysis and assessment of an advanced hydrogen liquefaction system." International Journal of Hydrogen Energy 43(2), (2018): 1139-1151.

[27] U. Cardella, L. Decker, and H. Klein. "Roadmap to economically viable hydrogen liquefaction." International Journal of Hydrogen Energy 42(19), (2017): 13329-13338.

[28] Mehmet Kanoglu, Ceyhun Yilmaz, and Aysegul Abusoglu. "Geothermal energy use in absorption precooling for Claude hydrogen liquefaction cycle." International Journal of Hydrogen Energy 41(26), (2016): 11185-11200.

[29] Majid Aasadnia, Mehdi Mehrpooya, and Bahram Ghorbani. "A novel integrated structure for hydrogen purification using the cryogenic method." Journal of Cleaner Production 278 (2021): 123872.

[30] Jiang Bian, Jian Yang, Yuxing Li, Zhaoqi Chen, Fachun Liang, and Xuewen Cao. "Thermodynamic and economic analysis of a novel hydrogen liquefaction process with LNG precooling and dual-pressure Brayton cycle." Energy Conversion and Management

250 (2021): 114904.

[31] Liang Yin and Yonglin Ju. "Process optimization and analysis of a novel hydrogen liquefaction cycle." International Journal of Refrigeration 110 (2020): 219-230.

[32] Jimena Incer-Valverde, Janis Mörsdorf, Tatiana Morosuk, and George Tsatsaronis. "Power-to-liquid hydrogen: Exergy-based evaluation of a large-scale system." International Journal of Hydrogen Energy (Available online 1 October 2021).

[33] Ceyhun Yilmaz. "Optimum energy evaluation and life cycle cost assessment of a hydrogen liquefaction system assisted by geothermal energy." International Journal of Hydrogen Energy 45(5), (2020): 3558-3568.

[34] Murat Koc, Nejat Tukenmez, and Murat Ozturk. "Development and thermodynamic assessment of a novel solar and biomass energy based integrated plant for liquid hydrogen production." International Journal of Hydrogen Energy 45(60), (2020): 34587-34607.

[35] Songwut Krasae-in, Jacob H. Stang, and Petter Neksa. "Exergy analysis on the simulation of a small-scale hydrogen liquefaction test rig with a multi-component refrigerant refrigeration system." International Journal of Hydrogen Energy 35(15), (2010): 8030-8042.

[36] Yunus Emre Yuksel, Murat Ozturk, and Ibrahim Dincer. "Energetic and exergetic assessments of a novel solar power tower based multigeneration system with hydrogen production and liquefaction." International Journal of Hydrogen Energy 44(26), (2019): 13071-13084.

[37] T. A. H. Ratlamwala, I. Dincer, M. A. Gadalla, and M. Kanoglu. "Thermodynamic analysis of a new renewable energy based hybrid system for hydrogen liquefaction." International Journal of Hydrogen Energy 37(23), (2012): 18108-18117.

[38] Hamed Rezaie Azizabadi, Masoud Ziabasharhagh, and Mostafa Mafi. "Introducing a proper hydrogen liquefaction concept for using wasted heat of thermal power plants-case study: Parand gas power plant." Chinese Journal of Chemical Engineering 40 (2021): 187-196.

[39] Zafer Utlu and Arif Karabuga. "Conventional and enhanced exergy analysis of a hydrogen liquefaction system." International Journal of Hydrogen Energy 46(2), (2021): 2296-2305.

[40] Mohamed A. Gadalla, Tahir Abdul Hussain Ratlamwala, Ibrahim Dincer, and Mehmet Kanoglu. "Performance assessment of an integrated absorption cooling–hydrogen liquefaction system using geothermal energy." International Journal of Exergy 12(2), (2013): 205-225.

[41] Hasan Ozcan and Ibrahim Dincer. "Thermodynamic modeling of a nuclear energy based integrated system for hydrogen production and liquefaction." Computers and Chemical Engineering 90 (2016): 234-246.

[42] F. Ahmadi Boyaghchi and A. Sohbatloo. "Exergetic, exergoeconomic, and exergoenvironmental assessments and optimization of a novel solar cascade organic Rankine cycle-assisted hydrogen liquefaction." Scientia Iranica B 28(1), (2021): 273-290.

[43] Zahra Alizadeh Afrouzy and Masoud Taghavi. "Thermo-economic analysis of a novel integrated structure for liquefied natural gas production using photovoltaic panels." Journal of Thermal Analysis and Calorimetry 145(3), (2021). 1509-1536.

[44] Azra Malik, Ahteshamul Haque, V S Bharath Kurukuru, Mohammed Ali Khan, and Frede Blaabjerg. "Overview of Fault Detection Approaches for Grid Connected Photovoltaic Inverters." e-Prime - Advances in Electrical Engineering, Electronics and Energy, (2022): 100035.

[45] Amirul Syafiq, Vengadaesvaran Balakrishnan, Mohd Syukri Ali, Sanjay J Dhoble, Nasrudin Abd Rahim, Azimah Omar, and Ab Halim Abu Bakar. "Application of transparent self-cleaning coating for photovoltaic panel: a review." Current Opinion in Chemical Engineering 36, (2022): 100801.

[46] Bahram Ghorbani, Gholamreza Salehi, Armin Ebrahimi, and Masoud Taghavi. "Energy, exergy and pinch analyses of a novel energy storage structure using post-combustion CO_2 separation unit, dual pressure Linde-Hampson liquefaction system, two-stage organic Rankine cycle and geothermal energy." Energy 233. (2021): 121051.

[47] Armin Ebrahimi, Bahram Ghorbani, and Masoud Taghavi. "Pinch and exergy evaluation of a liquid nitrogen cryogenic energy storage structure using air separation unit, liquefaction hybrid process, and Kalina power cycle." Journal of Cleaner Production 305. (2021): 127226.